Paresthesia Thresholds in Spinal Cord Stimulation: A Comparison of Theoretical Results with Clinical Data

Johannes J. Struijk, Jan Holsheimer, Giancarlo Barolat, Jiping He, and Herman B. K. Boom

Abstract— **The potential distributions produced in the spinal cord and surrounding tissues by dorsal epidural stimulation at the midcervical, midthoracic, and low thoracic levels were calculated with the use of a volume conductor model. Stimulus thresholds of myelinated dorsal column fibers and dorsal root fibers were calculated at each level in models in which the thickness of the dorsal csf layer was varied. Calculated stimulus thresholds were compared with paresthesia thresholds obtained from measurements at the corresponding spinal levels in patients. The influences of the csf layer thickness, the contact separation in bipolar stimulation and the laterality of the electrodes on the calculated thresholds were in general agreement with the clinical data.**

I. Introduction

In order to understand the immediate effects of epidural spinal cord stimulation (ESCS), the potential field produced by electrical stimulation and the response of neural elements in the spinal cord to the imposed field should be known. Therefore, modeling may be helpful to gain insight into the mechanisms underlying the phenomena observed in patients, to aid the development of new stimulation methods (e.g., the design of electrodes) and to provide guidelines for further research.

Only a few ESCS modeling studies have appeared in the literature. 2-D calculations of the potential field were carried out by Rusinko *et al.* [1], Coburn [2] and Sin and Coburn [3]. These calculations may be useful to investigate which geometrical parameters and tissue properties are the most critical. However, when the fields are applied to nerve fiber models 3-D solutions are indispensable.

Three-dimensional calculations were performed by Coburn and Sin [4] and Struijk *et al.* [5], whereas Swiontek *et al.* [6] did some field measurements in the spinal cord (post mortem). A major drawback in the latter work is that the stimulating current was applied using electrodes at the pial surface, thus bypassing the shunting cerebrospinal fluid (csf) which, according to the theoretical work [2]–[5], plays a major role in the current distribution.

Coburn [7] applied a calculated 3-D field to a cable model [8] of myelinated dorsal column (DC) fibers and myelinated dorsal root (DR) fibers. He found that the stimulus thresholds for these fibers were of the same order of magnitude as paresthesia thresholds observed in patients and that DR fibers had relatively low thresholds in comparison to DC fibers. This was partly confirmed by Struijk *et al.* [9]–[10] who calculated thresholds using a more realistic DC fiber model and various DR-fiber models as well.

The relatively low DR fiber thresholds could account for the occurrence of segmental effects, such as a band of tightness around the chest in midthoracic stimulation [11], presumably due to DR fiber activation. These modeling studies also predict that in case of a thin csf layer between electrode and spinal cord, thresholds of DC fibers and DR fibers are approximately the same, which might explain the observations that in some cases paresthesia was first perceived in the lower extremities [11] during cervical stimulation.

In the present study, models of ESCS, comprising volume conductor models of the spinal cord and surrounding tissues at midcervical, midthoracic and low thoracic vertebral levels, and models of DC fibers and DR fibers were used to simulate clinical data. The impedance between bipolar electrodes in the volume conductor models was adapted to the load impedances measured in patients. In this initial validation study the influences of the dorsal csf layer thickness, the contact separation in bipolar stimulation and the laterality of the electrodes on stimulus threshold were investigated. The calculated stimulus thresholds were compared with paresthesia thresholds measured in patients.

II. Methods

A. Volume Conductor Models

Three-dimensional volume conductor models of the spinal cord at midcervical, midthoracic, and low thoracic vertebral levels were used in this study. Transverse sections of these models are shown in Fig. 1. Each model comprises the spinal cord, which is composed of gray matter (gm) and white matter (wm), cerebrospinal fluid (csf), epidural space (es), vertebral bone (vb), a layer representing surrounding tissues (sl), electrode contact insulation (is) and a thin layer representing the dura mater (dm) at the dorsal side. The small dorsal root filaments, immersed in the well-conducting csf, were not incorporated in the volume conductor model [10].

The tissue conductivities used in the model are given in Table I. The values of the white matter, gray matter, epidural fat and vertebral bone were taken from Geddes and Baker [12]. We measured the csf conductivity at 37°C previously

Manuscript received October 12, 1992; revised July 27, 1993. This work was supported in part by a grant from Medtronic Inc., Minneapolis, MN.

J. J. Struijk, J. Holsheimer, and H. B. K. Boom are with the Department of Electrical Engineering, Institute for Biomedical Technology, University of Twente, 7500 AE Enschede, The Netherlands.

G. Barolat and J. He are with the Department of Neurosurgery, Jefferson Medical College, Thomas Jefferson University, Philadelphia, PA 19107.

IEEE Log Number 9212542.

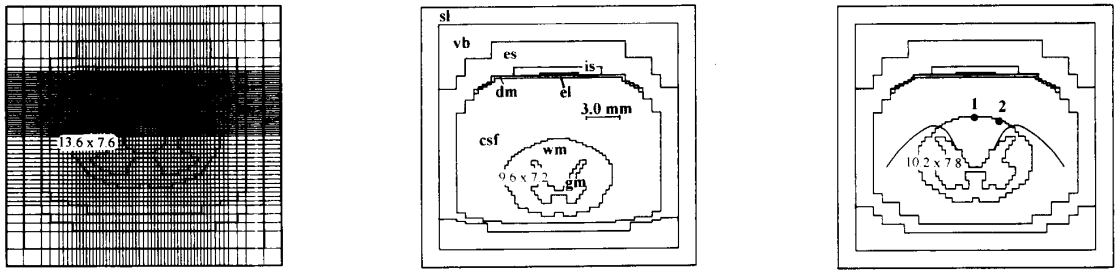

(a) (b) (c)

Fig. 1. Transverse sections of volume conductor models at three spinal levels with median valued dorsal csf layer thickness: (a) Midcervical level, the grid is shown; (b) Midthoracic level, sl = surrounding layer, vb = vertebral bone, es = epidural space, is = contact insulation, dm = dura mater, csf = cerebrospinal fluid, wm = white matter, gm = gray matter, el = electrode contact; (c) Low thoracic level, two dorsal roots and the positions of the dorsomedial DC fiber (1) and the dorsolateral DC fiber (2) are shown. In each figure the dimensions (lateral × dorsoventral) of the spinal cord are given in mm.

TABLE I
CONDUCTIVITIES (in S/m) OF THE VOLUME CONDUCTOR COMPARTMENTS

gm	gray matter	0.23
wm	white matter	0.60 longitudinal
		0.083 transverse
csf	cerebrospinal fluid	1.7
es	epidural space	0.04
dm	dura mater	0.03
vb	vertebral bone	0.04
sl	surrounding layer	0.004
is	electrode insulation	0.001

TABLE II
THICKNESS OF DORSAL csf LAYER [mm]; 95% CONFIDENCE INTERVALS IN PARENTHESES

Vertebral level	Median	25th%	75th%	Nr. subjects
Midcervical	2.3	2.0	3.3	16
	(2.0–3.3)	(1.5–2.2)	(2.2–3.7)	
Midthoracic	5.5	4.8	7.0	18
	(4.8–6.0)	(3.8–5.5)	(5.5–8.8)	
Low thoracic	3.5	2.5	5.0	17
	(2.5–4.0)	(2.0–3.0)	(3.0–6.5)	

in samples from three subjects [5]. The conductivity of the dura mater is unknown. Its model value was taken such that the total impedance between two contacts (10 mm center separation) matched the impedance measured bipolarly in patients (mean = $1091\Omega, sd = 346\Omega, n = 114$). Therefore, the dura impedance also includes the impedance of the tissue (connective tissue, epidural fat) which may be present between electrode and dura. In simulations of unipolar (cathodal) stimulation the boundary of the model serves as the distant contact. The conductivity of the surrounding layer (sl) was given a value such that the impedance between cathode and boundary matched the impedance measured unipolarly (mean = $715\Omega, sd = 229\Omega, n = 69$). In the model the impedance was obtained by calculating the currents at the surface of each contact.

The contacts were modeled as voltage sources (Dirichlet condition) because commercially available stimulators have voltage sources. The dimensions of the contacts were 3.6 × 3.6 mm, matching the contact areas of the Resume® lead (Medtronic, Inc., Minneapolis, MN). Bipolar configurations with center separations of 10, 20, 30, 40, and 50 mm and a unipolar configuration were used. Because of the different morphology distinct vertebral levels had to be modeled separately. In relation to the availability of clinical data the following vertebral levels were chosen: midcervical (C4–C6), midthoracic (T4–T7) and low thoracic (T10–T11).

The dorsal csf layer thickness at each level was estimated from an MRI study on healthy subjects (18 males, 20–40 years of age). The values of the median and the 25th and 75th percentiles are given in Table II. The 95% confidence intervals were calculated according to the method given in the Appendix, which is a modification of the method used to calculate the confidence interval of the median [13].

In Fig. 1 for each level a model is shown with the median value of the dorsal csf layer thickness at that level. Similar models were used with csf layer thicknesses equal to the 25th percentile and the 75th percentile of the MRI data (Table II). These models were used for simulating the clinical data. Because paresthesia thresholds had a non-Gaussian, skew distribution, the use of the median and the percentiles was preferred to the use of the mean and standard deviation to characterize the distributions.

The dimensions of the spinal cord are given in Fig. 1 and were taken from literature [14]–[20]. For the low thoracic level only a few data were available. The cord morphology at all three vertebral levels was taken from Fix [21]. The length of the model was 60 mm.

To discretize the volume conductor model, a rectangular grid was used [see Fig. 1(a)]. Grid spacings varied from 0.2 to 1.6 mm with the smallest values near the electrodes and the dorsal columns. The number of grid points was 185193 (57 × 57 × 57). A finite difference method (using Taylor series) was applied to discretize the governing Laplace equation. The resulting set of linear equations were solved using a Red–Black Gauss-Seidel iteration [22] with variable overrelaxation (overrelaxation after each red and each black sweep). Two solutions were calculated simultaneously, one starting with an underestimated initial solution and the other one with an overestimated initial solution. The overrelaxation factor was increased if the two solutions approached each other too slowly, whereas it was decreased if the difference between the solutions decreased too quickly, thereby avoiding

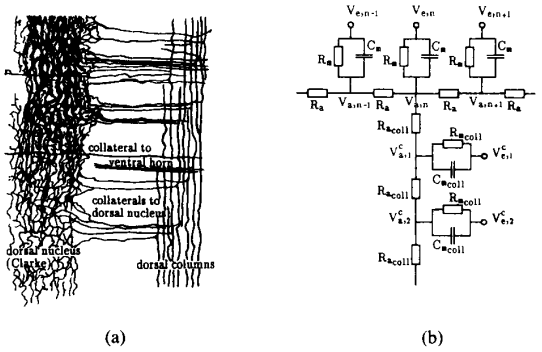

Fig. 2. Dorsal column fibers. (a) Rostrocaudal DC fibers issuing collaterals into the gray matter (adapted from Cajal [23]); (b) Network model consisting of a rostrocaudal fiber (horizontal part) and a collateral (vertical part); R_m: nodal membrane resistance, C_m: nodal membrane capacitance, R_a: internodal intracellular resistance, V_a: nodal intracellular potential, V_e: extracellular (applied) potential.

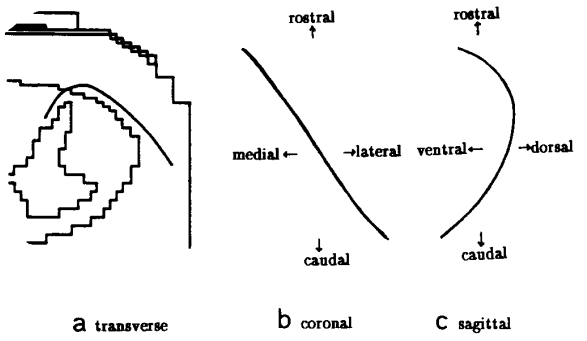

Fig. 3. Projections of the DR fiber on three orthogonal planes: (a) transverse plane; (b) coronal plane; (c) sagittal plane.

instability of the iteration process due to the overrelaxation. The calculations were finished when the average absolute difference between the two solutions was less than 0.01% of the average absolute value of the calculated field itself. For a special case including discontinuous conductivities, which could also be solved analytically, the numerical solutions appeared to be accurate within 2% [10].

B. Nerve Fiber Models

Two types of nerve fiber models were used: DR fibers and DC fibers. DC fibers are longitudinal fibers in the dorsal columns issuing collaterals into the dorsal gray matter [Fig. 2(a)] [23]–[25]. The model of these fibers is a cable model [8] in which the myelin is assumed to be a perfect insulator, extended with collaterals as shown in Fig. 2(b). All nodes were made excitable using the equations by Chiu *et al.* [26] transformed to a temperature of 37°C. The collaterals were attached to every second node of Ranvier of the main fiber. This model was described in detail in a previous paper and simulations indicated that the presence of collaterals reduces the stimulus threshold (the minimum stimulus amplitude at which a given fiber is exeited) by 30–50% [9]. A stimulus pulse width of 210 μs was used to calculate the stimulus thresholds of both DC and DR fibers.

For the DR fiber we used a cable model with a curved trajectory, the proximal end being connected to a DC fiber model. The curvature of the model is shown in Fig. 3. This model and its properties were described previously [10]. The fiber entered the spinal cord at a rostrocaudal level corresponding to the center of the cathode, at which position the stimulus threshold had the lowest value.

The fiber models were given diameters in the upper range of the diameter distribution of these fibers. We assumed that activation of the hair receptor fibers (A$\alpha\beta$ fibers [25]) is responsible for paresthesia perception, because they are the largest fibers and will thus have the lowest excitation thresholds. We used a DR fiber diameter of 15 μm. Assuming a linear relationship between propagation velocity and fiber diameter [27], the attached DC fiber was given a diameter of 12 μm, in accordance with Desmedt and Cheron [28] who found a drop in propagation velocity of about 19% after bifurcation of the DR fiber in the human dorsal columns.

The transverse position of the DR fiber in the volume conductor model is shown in Fig. 1(c). The positions of two DC fibers, indicated by 1, 2, are also shown. Fiber 1 has a dorsomedial position and is therefore assumed to be a fiber of sacral origin [24], [29], [30]. In accordance with Petit and Burgess [31], who found a decrease in propagation velocity of 40–65% along the ascending fibers in the dorsal columns of the cat, fiber 1 was given a diameter of 7.5 μm. This value corresponds to the upper range of fiber diameters in the human fasciculus gracilis as found by Ohnishi *et al.* [32] (up to 8 μm), although Häggqvist [33] found fiber diameters of more than 10 μm in this area. Fiber 2 represents a DC fiber close to the entry level of the corresponding DR fiber and had a 12 μm diameter. We will refer to these fibers as fiber DC1, DC2 and DR.

C. Collection of Clinical Data

The impedance values and paresthesia thresholds in ESCS were measured in patients with either an Itrel® or Itrel II® implanted pulse generator with a Resume® lead (Medtronic Inc., Minneapolis, MN). The 108 patients included in this study were suffering from either chronic pain or spasticity. The main aetiologies were reflex sympathetic dystrophy, low back pain and spinal cord injury. Paresthesia threshold was defined as the minimum voltage at which the patient perceived paresthesia (a tingling or buzzing sensation due to activation of afferent hair fibers), measured with the patient in the supine position at a repetition rate of 50 pps and a pulse width of 210 μs.

The stimulation amplitude was gradually increased starting from 0 V with increments of 0.25 V (Itrel®) or 0.1 V (Itrel II®) to detect paresthesia threshold. At each increment the patient was asked to report whether and where paresthesiae were perceived. Impedance was measured at 50 pps, a pulse width of 210 μs and an amplitude of 1.0 V using the impedance measurement option of the Itrel II® implantable pulse generator.

The Resume® lead is an array of four circular contacts embedded in a strip of flexible insulating material. The contacts have a diameter of 4.0 mm and a center separation of

TABLE III
MINIMUM THRESHOLDS AS A FUNCTION OF VERTEBRAL LEVEL IN BIPOLAR STIMULATION (10 mm contact separation); 95% CONFIDENCE INTERVALS OF THE MEDIAN OF THE MEASURED DATA IN PARENTHESES

	Calculated $V_{th}[V]$	Median of measured $V_{pt}[V]$	Nr. subjects
Midcervical	1.61	0.58 (0.51–0.74)	31
Midthoracic	4.20	1.40 (1.10–2.20)	24
Low thoracic	2.77	1.10 (0.86–1.30)	53

10 mm. The implanted lead has a rostrocaudal orientation. Measurements were carried out with a unipolar electrode configuration (the metal case of the pulse generator being the anode) and bipolar configurations with 10, 20, and 30 mm contact separations as well.

Data were obtained from patients having the electrodes placed between 0 and 3 mm lateral to radiological midline at the vertebral levels C4–C6 (31 patients), T4–T7 (24 patients) and T10–T11 (53 patients). The radiological midline is related to the spinous processes and does therefore not necessarily coincide with the (dorso-ventral) midline of the spinal cord. For each patient all paresthesia thresholds measured at one level and with one electrode configuration were averaged to obtain series of independent data for statistical analysis. Because the paresthesia threshold data were not Gaussian distributed the median and the 25th and 75th percentile were calculated. The 95% confidence intervals were established using the method given in the Appendix.

III. RESULTS

A. Paresthesia Threshold as a Function of Spinal Level

The dorsal csf layer thickness is a major parameter affecting the threshold stimulus for the excitation of nerve fibers in the spinal cord, because this layer determines the electrode-fiber distance [5], [10], [34]. Table II shows that at the midcervical level the dorsal csf layer thickness is smallest and therefore it is expected that paresthesia thresholds will have the lowest values at that level. We calculated the stimulus threshold V_{th} of the fibers DC1, DC2 and DR at the three levels in bipolar stimulation with a contact separation of 10 mm and a dorsal csf layer thickness being the median of the measured values (Table II). The minimum values of V_{th}, being V_{th} of the DR filter in all cases, are summarized in Table III. In the midcervical model with median csf layer thickness the values of the fibers DC1 and DC2 were about 100 and 50% higher, respectively. At midthoracic and low thoracic levels these differences were even more pronounced. Therefore, the expected recruitment order is DR fiber, lateral DC fiber and medial DC fiber successively.

For very small csf layer thicknesses (less than 1.0 mm) this order was reversed. In Table III the median of the measured paresthesia threshold (V_{pt}) and its 95% confidence interval are also given.

The model predicts relatively high V_{th} values in comparison to the measured V_{pt} values. However, the ratio V_{th}/V_{pt} is consistent at all three levels (2.78, 3.00, and 2.52 for midcervical, midthoracic, and low thoracic levels, respectively). There may be several causes for the discrepancy between calculated and measured thresholds (see Discussion).

B. Paresthesia Threshold as a Function of csf-Layer Thickness

We calculated the effect of csf layer thickness on threshold and compared the variation in calculated thresholds due to the variation in csf layer thickness with the observed variation in paresthesia thresholds, measured with the patients in supine position. Because the dorsal csf thicknesses of the patients were not measured and consequently unknown, this comparison only makes sense if it is assumed that differences in paresthesia thresholds are mainly due to differences in dorsal csf layer. We indeed made this assumption on the basis of the results on the relationship between paresthesia threshold and spinal level, and the high sensitivity of thresholds to a patient's position.

It is well known that paresthesia threshold varies with a patient's position. A supine position yields lower thresholds than an upright position. In cervical stimulation the set of the head strongly influences threshold. Both the patient's position and the set of the head affects the dorsal csf layer thickness. In the model we used csf layer thickness values equal to the median, the 25th and the 75th percentiles of the measures data at each vertebral level (Table II). We calculated V_{th} for fibers DC1, DC2, and DR using bipolar stimulation with a contact separation of 10 mm. The results for the DR fiber, normalized to the values with median csf layer thickness, are shown in Fig. 4 (bars). In all cases fiber DR had the lowest V_{th} value, although in the midcervical model with a 25th percentile csf layer thickness fibers DC1 and DC2 had only slightly higher values (40 and 20%, respectively).

In Fig. 4 the median and the 25th and 75th percentiles of the measured paresthesia thresholds V_{pt} normalized to the median values are also presented, together with the upper and lower limits of the 95% confidence intervals (markers). A comparison of the calculated values with the clinical data shows that their variations are in good agreement (although the calculated variations are slightly smaller at average), supporting the assumption that the variation of measured paresthesia threshold can be attributed mainly to the variation of csf layer thickness.

C. Paresthesia Threshold as a Function of Contact Separation

We calculated the stimulus thresholds V_{th} of fibers DC1, DC2, and DR in the three volume conductor models with median csf-layer thickness and contact separations of 10–50 mm, with steps of 10 mm and a unipolar configuration as well. The DR fiber again had the lowest V_{th} values. These values (except for the 40 and 50 mm separation), normalized to V_{th} at 10 mm contact separation are summarized in Fig. 5 (bars). These data show that in bipolar stimulation the model predicts that for DR fibers a minimum V_{th} occurs at a contact separation of about 20 mm. Simulations with 30, 40, and 50 mm contact separation showed a continuous slight increase of V_{th} (11% increase from 30 mm to 50 mm). For DC fibers however, minimum V_{th} occurred below 10 mm

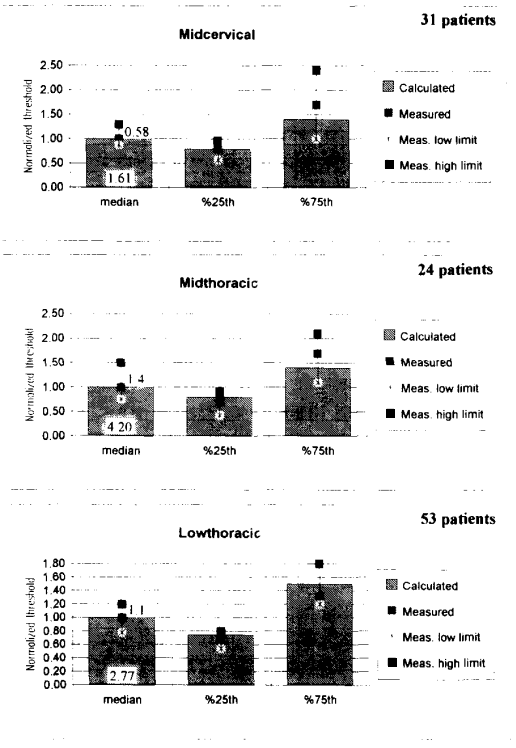

Fig. 4. Bars: Normalized calculated minimum thresholds (of DR fiber) versus dorsal csf layer thickness (median, 25th and 75th percentiles) at midcervical, midthoracic, and low thoracic levels. Absolute values are given in the bars (Bipolar, 10 mm contact separation). Markers: Normalized median, 25th and 75th percentiles of the measured paresthesia thresholds with the upper and lower limits of their 95% confidence intervals. Absolute values are given right to the central markers.

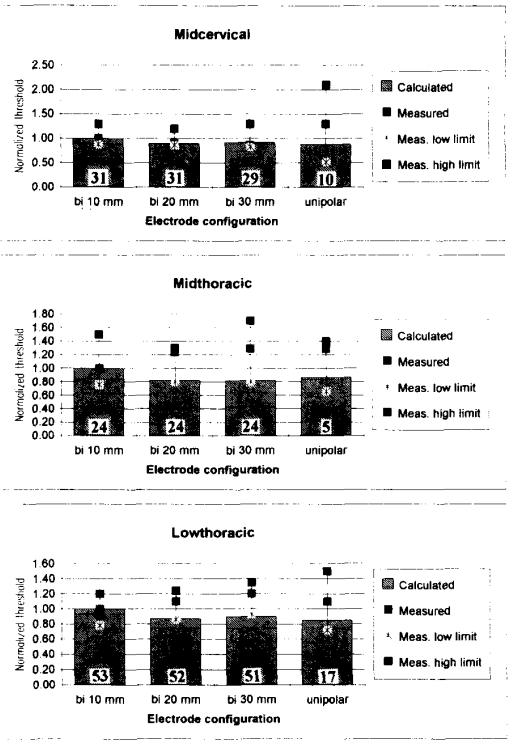

Fig. 5. Bars: Normalized calculated minimum thresholds (of DR fiber) as a function of contact separation at midcervical, midthoracic and low thoracic levels. Markers: Normalized median values of the measured paresthesia thresholds with the upper and lower limits of their 95% confidence intervals; the number of data is given at the bottom of each bar.

contact separation as we have shown previously [34], [35]. For fiber DC1 at the midcervical level normalized V_{th} values were 100% (3.37 V), 112%, and 117% for 10, 20, and 30 mm contact separation, respectively, whereas for fiber DC2 these values were 100% (2.56 V), 114% and 119%. So, in our model, we found that with increasing contact separation (up to 50 mm), the ratio $V_{th}(\mathrm{DR})/V_{th}(\mathrm{DC})$ decreases, thus increasing the preferential stimulation of DR fibers. The highest preference to DR fibers was obtained in unipolar stimulation.

Barolat *et al.* [11] found that overall paresthesia threshold increased slightly as the contact separation was increased from less than 30 mm to more than 50 mm, whereas the percentage of body area covered by paresthesia decreased with increasing contact separation. This is well in accordance with our theoretical results if we assume that in dorsal root stimulation a smaller percentage of body area will be covered by paresthesia than in dorsal column stimulation, in which case fibers originating from lower spinal levels are activated as well.

Because of the relatively large confidence intervals the measurement data as shown in Fig. 5 (markers) do not show a significant change (Kruskal–Wallis test [13], $p = 0.05$) of paresthesia threshold as contact separation is increased from 10 mm to 30 mm (see [11] for larger distances). The slight minimum which occurred at 20 mm in the calculated V_{th} was not observed in the experimental data.

In the model, unipolar stimulation resulted in a relatively low V_{th}. The measurement data for unipolar stimulation show large confidence intervals due to the small number of patients in which unipolar measurements were performed (10, 5, and 17 patients at the midcervical, midthoracic and low thoracic level, respectively).

D. Influence of the Lateral Position of the Electrode Contacts

According to Barolat *et al.* [11] thresholds and paresthesia distributions are largely affected by the laterality of the contacts. They measured an average paresthesia threshold of 1.7 V for all bipolar combinations with contacts within 3 mm of the radiological midline at thoracic vertebral levels. The average threshold dropped to 1.2 V (70%) for contacts at 3–5 mm from the midline and 0.8 V (47%) for contacts at more than 5 mm from midline. This effect is most likely related to dorsal root stimulation. With both contacts at one side at 0.5 to 3 mm from midline (see Fig. 6), most paresthesia distributions were unilateral. When the anode was more than 0.5 mm from midline contralateral to the cathode, bilateral paresthesia distributions slightly increased. However, the position of the cathode was the most critical [11].

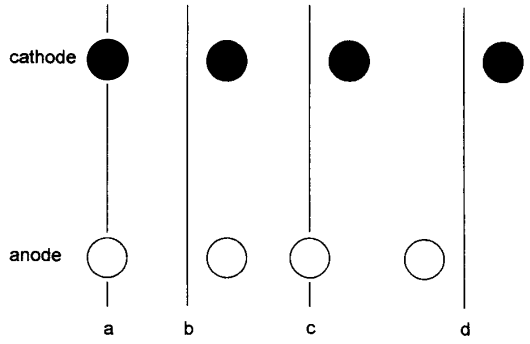

Fig. 6. Positions of the contacts in a coronal plane. (a) Contacts at midline; (b) contacts at the same side; (c) cathode lateral, anode at midline; (d) contacts at opposite sides.

TABLE IV
CALCULATED THRESHOLDS ($V_{th}[V]$), FOR EACH FIBER NORMALIZED TO VALUES WITH BOTH CONTACTS AT MIDLINE, AS A FUNCTION OF LATERALITY OF THE CONTACTS. BIPOLAR STIMULATION (10 mm contact separation), MIDTHORACIC MODEL

	DC1	DC2-left	DC2-right	DR-left	DR-right
Contacts midline	1.0	1.0	1.0	1.0	1.0
	(13.9 V)	(10.0 V)	(10.0 V)	(4.20 V)	(4.20 V)
Contacts same side	1.44	1.72	0.86	1.81	0.80
Cathode lateral	1.41	1.64	0.90	1.76	0.83
Contacts opposite sides	1.40	1.60	0.94	1.68	0.85

In order to assess the relative influence of the anodal and cathodal position we did four simulations (see Fig. 6): (1) both contacts at midline, (2) both contacts at 3.0 mm from midline at the right side, (3) cathode at 3.0 mm from midline at the right side and anode at midline, (4) cathode at 3.0 mm at the right side and anode at 3.0 mm left to midline. The midthoracic model was used with medial dorsal csf layer thickness (5.5 mm) and 10 mm contact separation. The fibers used were DC1, DC2-left, DC2-right, DR-left and DR-right, with left and right fibers mirrored with respect to midline.

In Table IV the results, normalized to the results with both contacts at midline, are summarized. The data show that the clinical results can be explained with the model, assuming that DR fibers play a prominent role. The cathodal position is more critical than the anodal one, but V_{th} still slightly decreases if the anode is moved towards the side of the corresponding fiber (see also Holsheimer and Struijk [34]). When the electrodes are at the same side at 3 mm from midline, the model predicts a minimum threshold of 80% (DR fiber) compared with the situation where both electrodes are at midline. This is in good agreement with the measured data (70%) for electrodes at 3–5 mm from midline [11].

IV. DISCUSSION

In this investigation the calculated threshold voltages for the activation of DC and DR fibers of the spinal cord with epidural electrical stimulation were compared with measured paresthesia thresholds in patients. We assumed that these myelinated primary afferent fibers are involved in ESCS and that paresthesiae, at threshold levels, are directly related to activation of these fibers without modulation by excitatory or inhibitory spinal or long loop circuits. At stimulus amplitudes beyond threshold, relations may be more complex.

We found a discrepancy between paresthesia thresholds and calculated stimulus thresholds, the latter being 252–300% of the measured values (Table III), whereas Coburn seemed to have obtained a better fit between the modeling results and measured paresthesia thresholds [7]. However, he compared thresholds obtained with a model with a dorsal csf thickness of 1.75 mm, with thresholds measured at midthoracic and high thoracic levels [36], where in reality the median of the csf layer thickness is about three times larger. We calculated, that the difference between thresholds for a 1.75 mm csf layer and a 5 mm csf layer is more than a factor 3. Therefore, Coburn's results show the same discrepancy between modeling and clinical data as ours.

The discrepancy between calculated and measured thresholds may be due to variability of parameters in both the nerve fiber models and the volume conductor models. The geometrical and electrical parameters of mammalian myelinated nerve fibers are described in literture [8], [27], [37]. In our fiber models average parameter values were used [9]. However, most parameters have large standard deviations and therefore, the threshold stimulus of fibers with a given diameter and a given position may vary largely. Wide physiological ranges have been observed for, amongst others, the ratio of the internodal length and the fiber diameter (L/D), ratio of axon diameter and outer fiber diameter, nodal membrane capacitance, nodal membrane conductivity, intra axonal conductivity and length of the node of Ranvier [27], [37]. We calculated (unpublished results) a threshold stimulus distribution of a fiber model where those parameters were given a normal distribution with standard deviations of 20% of their average values (from data in the literature we calculated a standard deviation being 26% of the average value of L/D). We found that about 5% of the distribution was below half of the median threshold value of the distribution and it may be assumed that this 5% (or even less) of "low threshold" fibers defines the threshold of the whole fiber population (of given diameter) in the dorsal columns or dorsal roots. The parameter variability will thus significantly decrease the threshold of a population of nerve fibers in the spinal cord or in the dorsal roots.

The variability of the membrane capacitance hardly had any influence, because of the relatively long pulse (210 μs). A parameter of the volume conductor model which strongly affects stimulus thresholds, is the dorsal csf layer thickness [5]. The number of MRI scan data used to estimate this parameter was relatively small, thus giving rise to the possibility of large errors in the estimates (large confidence intervals, see Table II). The insertion of a relatively large electrode lead in the narrow epidural space will indent the dura, thus decreasing the csf layer thickness and decreasing paresthesia threshold. Another geometrical factor giving rise to a relatively low measured paresthesia threshold is the fact that the electrode position was up to 3 mm off midline.

The modeling results show that variations in csf layer thickness can largely account for the variability of the measured paresthesia thresholds among patients. One would expect the impedance also to affect V_{pt}. However, no statistically significant relationship was found between measured impedance and V_{pt}. The influence of the impedance variability on V_{pt} might be overshadowed by the variations in csf layer thickness. In the model the csf layer thickness changes only caused less than 4% variations of the calculated impedance, so within the physiological range, csf layer thickness and impedance are hardly correlated.

Paresthesia usually starts in the dermatomes corresponding to the spinal level of the cathode [38] and often spreads caudally with increasing stimulus intensity [11]. This behavior is consistent with the model prediction that recruitment starts in the dorsal roots and spreads into the lateral and the medial dorsal columns with increasing amplitude. Sometimes, paresthesia starts at a lower level which can be explained by a reverse recruitment order as obtained in the midcervical model with a small dorsal csf layer thickness.

From this initial validation study it can be concluded that a consistent discrepancy exists between the absolute values of the calculated threshold stimuli and the measured paresthesia thresholds at all three spinal levels. Further improvement of the model is needed to eliminate this discrepancy. Therefore, reliable data on the spread of some model parameters, such as the dorsal csf layer thickness in patients with implanted electrodes and nerve fiber parameters are needed. On the other hand, the change in calculated threshold values as a function of csf layer thickness, contact separation and laterality were in general agreement with both the clinical measurements and the predicted spread of paresthesia. The model may therefore be used to predict the effects of various electrode configurations. The influence of contact dimensions, electrode position and contact combination on the stimulus threshold of DC fibers and DR fibers can be assessed with the model. Other neural elements, such as fibers in the dorsolateral funiculus and dorsal horn cells can be incorporated into the model. The method described in this paper may thus be a useful tool for designing new electrodes which will make it possible to activate various neural pathways or structures in a more specific way.

V. Appendix

A. Confidence Interval of the 100p th Percentile Using the Sign Test

The confidence interval of the estimated 100pth percentile of a random sample $X = X_1, X_2, \cdots, X_n$ of nonparametric data can be obtained using the Sign test (for the 25th percentile, the median and the 75th percentile $p = 0.25, p = 0.5, p = 0.75$, respectively).

Let Π be the 100pth percentile of a random sample X.

Test the null hypothesis $H_0 : \Pi = \Pi_0$

against the alternative $H_1 : \Pi \neq \Pi_0$

using the Sign test statistic S = number of X_i for which $X_i < \Pi_0, i = 1, \cdots, n$. Then S has a binomial distribution [21] because the probability of $X_i < \Pi_0$ equals p under the assumption H_0. Thus, $P(S = s) = B(s, n, p) = \binom{n}{s} \cdot p^s \cdot (1-p)^{n-s}$, for $s = 0, 1, 2, \cdots, n$. H_0 is rejected at level α if $S \leq s_1$ or if $S \geq s_2$ where s_1 and s_2 follow from:

$$P[S \leq s_1] = \alpha/2$$
$$P[S \geq s_2] = \alpha/2$$

The latter can be rewritten as $P[S \leq s_2 - 1] = 1 - \alpha/2$.

For given n, α and p, the values of s_1 and $s_2 - 1$ can be obtained from a table of the binomial distribution.

Repeating this test procedure for all possible values of Π_0 a $100 \cdot (1-\alpha)\%$ confidence interval is then the range of values Π_0 so that S is in the acceptance region. If the observations $X_1, X_2, \cdots, X_n$ are ordered from smallest to largest, the confidence interval becomes

$$X_{s1} + 1 \text{ to } X_{s2}.$$

References

[1] J. B. Rusinko, C. F. Walker, and N. G. Sepulvedo, "Finite element modeling of potentials within the human thoracic spinal cord due to applied electrical stimulation," *Frontiers of Engineering in Health Care*, vol. 3, in *Proc. IEEE-EMBS Conf.*, Houston, TX, 1981, pp. 76–81.

[2] B. Coburn, "Electrical stimulation of the spinal cord: Two-dimensional finite element analysis with particular reference to epidural electrodes," *Med. Biol. Eng. Comp.*, vol. 18, pp. 573–584, 1980.

[3] W. K. Sin and B. Coburn, "Electrical stimulation of the spinal cord: A further analysis relating to anatomical factors and tissue properties," *Med. Biol. Eng. Comp.*, vol. 21, pp. 264–269, 1983.

[4] B. Coburn and W. K. Sin, "A theoretical study of epidural electrical stimulation of the spinal cord—Part I: Finite element analysis of stimulus fields," *IEEE Trans. Biomed. Eng.*, vol. BME-32, pp. 971–977, 1985.

[5] J. J. Struijk, J. Holsheimer, B. K. van Veen, and H. B. K. Boom, "Epidural spinal cord stimulation: Calculation of field potentials with special reference to dorsal column nerve fibers," *IEEE Trans. Biomed. Eng.*,vol. 38, pp. 104–110, 1991.

[6] T. J. Swiontek, A. Sances, S. J. Larson, J. J. Ackmann, J. F. Cusick, G. A. Meyer, and E. A. Miller, "Spinal cord implant studies," *IEEE Trans. Biomed. Eng.*, vol. BME-23, pp. 307–312, 1976.

[7] B. Coburn, "A theoretical study of epidural electrical stimulation of the spinal cord—Part II: Effect on long myelinated fibers," *IEEE Trans. Biomed. Eng.*, vol. BME-32, pp. 978–986, 1985.

[8] D. R. McNeal, "Analysis of a model for excitation of myelinated nerve," *IEEE Trans. Biomed. Eng.*, vol. BME-23, pp. 329–337, 1976.

[9] J. J. Struijk, J. Holsheimer, G. G. van der Heide, and H. B. K. Boom, "Recruitment of dorsal column fibers in spinal cord stimulation: Influence of collateral branching," *IEEE Trans. Biomed. Eng.*, vol. 39, pp. 903–912, 1992.

[10] J. J. Struijk, J. Holsheimer, and H. B. K. Boom, "Excitation of dorsal root fibers in spinal cord stimulation: A theoretical study," *IEEE Trans. Biomed. Eng.*, in press.

[11] G. Barolat, S. Zeme, and B. Ketcik, "Multifactorial analysis of epidural spinal cord stimulation," *Stereotact. Funct. Neurosurg.*, vol. 56, pp. 77–103, 1991.

[12] L. A. Geddes and L. E. Baker, "The specific resistance of biological material—A compendium of data for the biomedical engineer and physiologist," *Med. Biol. Eng.*, vol. 5, pp. 271–293, 1967.

[13] G. K. Bhattacharyya and R. A. Johnson, *Statistical concepts and methods.* New York: Wiley 1977.

[14] C. H. Elliott, "Cross-sectional diameters and areas of the human spinal cord," *Anat. Rec.*, vol. 93, pp. 287–293, 1945.

[15] L. Nordqvist, "The sagittal diameter of the spinal cord and subarachnoid space in different age groups: A roentgenographic post-mortem study," *Acta Radiologica*, suppl. 227, pp. 1–96, 1964.

[16] L. Penning, J. T. Wilmink, H. H. van Woerden, and E. Knol, "CT-myelographic findings in degenerative dosorders of the cervical spine: Clinical significance," *Amer. J. Radiol.*, vol. 146, pp. 793–801, 1986.

[17] H. O. M. Thijssen, A. Keyser, M. W. M. Horstink, and E. Meijer, "Morphology of the cervical spinal cord on computed tomography," *Neuroradiol.*, vol. 18, pp. 57–62, 1979.

[18] I. O. Skalpe and O. Sortland, "Cervical myelography with metrazimide (amipaque)," *Neuroradiol.*, vol. 16, pp. 275–278, 1978.

[19] Y. L. Yu, G. H. du Boulay, J. M. Stevens, and B. E. Kendall, "Morphology and measurements of the cervical spinal cord in computer assisted myelography," *Neuroradiol.*, vol. 27, pp. 399–402, 1985.
[20] G. di Chiro and R. L. Fisher, "Contrast radiography of the spinal cord," *Arch. Neurol.*, vol. 11, pp. 125–143, 1964.
[21] J. D. Fix, *Atlas of the Human Brain and Spinal Cord.* Rockville, MD: Aspen Publishers, 1987.
[22] G. Dahlquist and O. Björk, *Numerical methods.* Englewood Cliffs, NJ: Prentice Hall, 1974.
[23] R. y Cajal, "Histologie du système nerveux de l'homme et de vertebrés, I", Paris, France, 1909.
[24] S. T. Bok, "Das-Zentralnervensystem: Das Rueckenmarck," in *Handbuch der mikroskopischen Anatomie des Menschen,* vol. 4, Berlin, Verlag von Julius Springer, 1928, pp. 478–578.
[25] R. E. W. Fyffe, "Afferent fibers," in *Handbook of the Spinal Cord,* vols. 2 & 3, R. A. Davidoff, Ed. *Anatomy and Physiology.* New York, Dekker, pp. 79–136, 1984.
[26] S. Y. Chiu, J. M. Ritchie, R. B. Rogart, and D. Stagg, "A quantitative description of membrane currents in rabbit myelinated nerve," *J. Physiol.*, vol. 292, pp. 149–166, 1979.
[27] S. G. Waxman, Ed., *Physiology and pathobiology of axons.* New York: Raven, 1978.
[28] J. E. Desmedt and G. Cheron, "Central somatosensory conduction in man: Neural generators and interpeak latencies of the far field components recorded from neck and right or left scalp and ear lobes," *Electroenceph. Clin. Neurophysiol.*, vol. 50, pp. 382–403, 1980.
[29] A. E. Walker and T. A. Weaver, "The topical organization and termination of the fibers of the posterior columns in Macaca mulatta," *J. Comp. Neurol.*, vol. 76, pp. 145–158, 1942.
[30] M. C. Smith and P. Deacon, "Topographical anatomy of the posterior columns of the spinal cord in man: The long ascending fibers," *Brain,* vol. 107, pp. 671–698, 1984.
[31] D. Petit and P. R. Burgess, "Dorsal column projection of receptors in cat hairy skin supplied by myelinated fibers," *J. Neurophysiol.*, vol. 31, pp. 849–855, 1968.
[32] A. Ohnishi, P. C. O'Brien, H. Okazaki, and P. J. Dyck, "Morphometry of myelinated fibers of fasciculus gracilis of man," *J. Neurol. Sci.*, vol. 27, pp. 163–172, 1976.
[33] G. Häggqvist, "Analyse der Faserverteilung in eineum Rückenmarck—Querschnitt (Th3)," Zeitschrift f. mikr.-anat. Forschung, vol. 39, pp. 1–34, 1936.
[34] J. Holsheimer and J. J. Struijk, "How do geometric factors influence epidural spinal cord stimulation? A quantitative analysis by computer modeling," *Stereotact. Funct. Neurosurg.*, vol. 56, pp. 234–249, 1991.
[35] J. Holsheimer, J. J. Struijk, and N. J. M. Rijkhoff, "Contact combinations in epidural spinal cord stimulation. A comparison by computer modeling," *Stereotact. Funct. Neurosurg.*, vol. 56, pp. 220–233, 1991.
[36] D. T. Jobling, R. C. Tallis, E. M. Sedgwick, and L. S. Illis, "Electronic aspects of spinal-cord stimulation in multiple sclerosis," *Med. Biol. Eng. Comp.*, vol. 18, pp. 48–56, 1980.
[37] F. Rattay, *Electrical Nerve Stimulation: Theory, Experiments and Applications.* New York: Springer-Verlag, 1990.
[38] M. R. Dimitrijevic, J. Faganel, P. C. Sharkey, and A. M. Sherwood, "Study of sensation and muscle twitch responses to spinal cord stimulation," *Int. Rehab. Med.*, vol. 2, pp. 76–81, 1980.

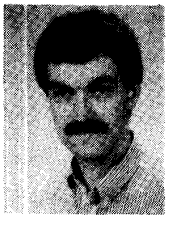

Johannes J. Struijk was born in Rijssen, The Netherlands, in 1963. He received the M.Sc. degree in electrical and biomedical engineering in 1988 and the Ph.D. degree in electrical engineering in 1992, from the University of Twente, Enschede, The Netherlands. Since 1992 he has been working as a post doctoral fellow in the Biomedical Engineering Division, Department of Electrical Engineering at the University of Twente.

His research interests are related to spinal cord stimulation and nerve stimulation, and involve volume conduction and neural modeling.

Jan Holsheimer was born in Enschede, The Netherlands, in 1941. He received the M.Sc. degree in biology and biophysics from the University of Groningen, The Netherlands, in 1965 and the Ph.D. degree in biomedical engineering from the University of Twente, Enschede, in 1982. In 1965 he joined the Biomedical Engineering Division, Department of Electrical Engineering at the University of Twente.

His research interests are volume conduction and the analysis of field potentials in the brain and electrical stimulation of nervous tissue.

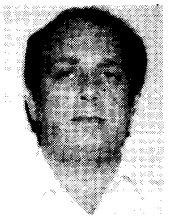

Giancarlo Barolat was born in Torino, Italy. He received the medical degree in 1974.

He undertook two consecutive residencies in Neurosurgery, respectively, at the University of Torino and at the Medical College of Wisconsin. He also served as a fellow in Neurosurgery at the Mount Sinai Medical Center, Miami, FL, and as a fellow in spinal cord injury at the Veterans Hospital in Wood, WI. He is a Diplomate of both the Italian and the American Board of Neurosurgery.

Dr. Barolat is currently Associate Professor of Neurosurgery, Director of the Division of Functional Neurosurgery and Director of the Neuro-Implant Program at Thomas Jefferson University, Philadelphia, PA.

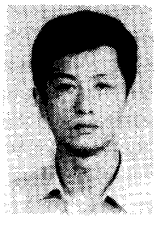

Jiping He was born in Shanghai, China. He received the B.S. degree from Huazhong University of Science and Technology, Wuhan, China, and the M.S. and Ph.D. degrees from the University of Maryland, College Park, MD, in 1982, 1984, and 1988, respectively.

After two years as a postdoctoral fellow at Artificial Intelligence Laboratories and Brain and Cognitive Sciences Department of Massachusetts Institute of Technology. He joined the faculty of Jefferson Medical College of Thomas Jefferson University, Philadelphia in the Fall, 1990. He is now Assitant Professor of departments of Neurosurgery and Physical Therapy. He also holds Adjunct Professor at Electrical Engineering, Temple University since 1992. He has publications in engineering, physiology and clinical journals on topics related to control, dynamics, and modeling on robotics, sensorimotor systems, on spinal cord stimulation for the treatment of pain and motor disorders, and on biomechanics and locomotion.

Herman B. K. Boom was trained as a Medical Physicist at the University of Utrecht, The Netherlands, where he received the Ph.D. degree in 1971.

He joined the Departments of Medical Physics and Medical Physiology where he was engaged in research in the field of cardiac mechanics and taught physiology and biophysics. Since 1976 he has held the Chair of Medical Electronics in the Department of Electrical Engineering, University of Twente, The Netherlands. His research interests are cardiovascular system dynamics, bioelectricity, and rehabilitation technology.